ЖЭТФ, 2011, том 139, вып. 3, стр. 440–445

ANALYTIC APPROACH TO THE APPROXIMATE SOLUTION OF THE INDEPENDENT DGLAP EVOLUTION EQUATIONS WITH RESPECT TO THE HARD-POMERON BEHAVIOR

B. Rezaei**, *G. R. Boroun**

Physics Department, Razi University
67149, Kermanshah, Iran

Received April 22, 2010

We show that it is possible to use hard-Pomeron behavior to the gluon distribution and singlet structure function at low x. We derive a second-order independent differential equation for the gluon distribution and the singlet structure function. In this approach, both singlet quarks and gluons have the same high-energy behavior at small x. These equations are derived from the next-to-leading order DGLAP evolution equations. All results can be consistently described in the framework of perturbative QCD, which shows an increase of gluon distribution and singlet structure functions as x decreases.

The Dokshitzer–Gribov–Lipatov–Altarelli–Parisi (DGLAP) evolution equations [1] are fundamental tools in the study of the Q^2 and x evolutions of structure functions, where x is the Bjorken scaling and Q^2 is the four-momenta transfer in deep inelastic scattering (DIS) processes [2]. The measurements of the $F_2(x,Q^2)$ structure functions by DIS processes in the small-x region have opened up a new era in parton density measurements inside hadrons. The structure functions reflect the momentum distributions of partons in a nucleon. It is also important to know the gluon distribution inside a hadron at low x because gluons are expected to be dominant in this region. The steep increase in $F_2(x,Q^2)$ towards low x observed at hadron-electron ring accelerator (HERA) also indicates a similar increase in the gluon distribution towards low x in perturbative quantum chromodynamics (PQCD). In the usual procedure, the DIS data are analyzed by the next-to-leading order QCD fits based on the numerical solution of the DGLAP evolution equations, and it is found that the DGLAP analysis can describe the data well in the perturbative region $Q^2 \geq 1$ GeV^2 [3]. As an alternative to the numerical solution, we can study the behavior of quarks and gluons through analytic solutions of the evolution equations. Although exact analytic solutions of the DGLAP equations are not possible in the entire range of x and Q^2, such solutions are possible under certain conditions [4,5] and are then quite successful as far as the HERA small-x data are concerned.

Small-x behavior of structure functions for fixed Q^2 reflects the high-energy behavior of the virtual Compton scattering total cross section with increasing the total center-of-mass energy squared W^2 because

$$W^2 = Q^2(1/x - 1).$$

The appropriate framework for the theoretical description of this behavior is the Regge-pole exchange picture [6]. It can be confidently asserted that the Regge theory is one of the most successful approaches to the description of high-energy scattering of hadrons. This high-energy behavior can be described by two contributions: an effective Pomeron with its intercept slightly above unity (~ 1.08) and the leading meson Regge trajectories with the intercept $\alpha_R(0) \approx 0.5$ [7]. The hypothesis of the Pomeron with data of the total cross section shows that a better description is achieved in alternative models with the Pomeron having unit intercept, but with a harder j singularity (a double pole) [8]. This model has two Pomeron components, each with the intercept $\alpha_P = 1$; one is a double pole and the other one is a simple pole [9]. It is tempting, however, to explore the possibility of obtaining approximate analytic solutions of the DGLAP equations themselves in the restricted domain of low x at least. Approximate solutions of the DGLAP equations have been reported [10–12] with

*E-mail: brezaei@razi.ac.ir
**E-mail: boroun@razi.ac.ir

considerable phenomenological success. Such an approximate scheme involves a Taylor expansion, valid at low x, and rephrases the DGLAP equations as partial differential equations in x and Q^2, which can be solved by standard methods.

In the past three decades, some authors reported a detailed analysis of the Regge input to the DGLAP equations [13–15]. We have shown [16–19] that it was possible to use Regge-like behavior as an input for the DGLAP evolution equations at low x. The small-x region of the deep inelastic electron–proton scattering offers a unique possibility to explore the Regge limit of PQCD [6]. This model gives the following parameterizations of the DIS distribution functions:

$$f_i(x,Q^2) = A_i(Q^2)x^{-\lambda_i}$$

($i = \Sigma$ (singlet structure function) and g (gluon distribution)), where λ_i is the Pomeron intercept minus one; it follows that

$$\lambda_i = \frac{d\ln f_i(x,Q^2)}{d\ln(1/x)}$$

definitely increases with Q^2. In this paper, we concentrate on the Regge behavior, although good fits to the results clearly show that the gluon distribution and the singlet structure function require a model with a hard Pomeron. In this scheme, this behavior, valid at low x, is used, and the DGLAP evolution equations are rephrased as independent partial differential equations in x and Q^2, which can be solved by standard methods. Also, we should be able to calculate λ_s and λ_g in the next-to-leading order (NLO) DGLAP equations.

The NLO DGLAP equations for the evolution of the singlet structure function and the gluon distribution can be written as

$$\begin{aligned}
\frac{dG(x,Q^2)}{d\ln Q^2} &= \frac{\alpha_s}{2\pi}\times\\
&\times\int\limits_0^{1-x} dz\left[P_{gg}^{LO+NLO}(1-z)G\left(\frac{x}{1-z},Q^2\right)+\right.\\
&\left.+P_{gq}^{LO+NLO}(1-z)\Sigma\left(\frac{x}{1-z},Q^2\right)\right],\\
\frac{d\Sigma(x,Q^2)}{d\ln Q^2} &= \frac{\alpha_s}{2\pi}\times\\
&\times\int\limits_0^{1-x} dz\left[P_{qq}^{LO+NLO}(1-z)\Sigma\left(\frac{x}{1-z},Q^2\right)+\right.\\
&\left.+2n_f P_{qg}^{LO+NLO}(1-z)G\left(\frac{x}{1-z},Q^2\right)\right],
\end{aligned} \tag{1}$$

where

$$G(x,Q^2) = xg(x,Q^2), \quad \Sigma(x,Q^2) = \frac{18}{5}F_2^{ep}(x,Q^2)$$

(at small x, the nonsinglet contribution $F_2^{ns}(x,Q^2)$ is negligible and can be ignored). In the evolution kernels and the running coupling, we take $N_f = 4$ (the number of active flavors); for simplicity, we also ignore the threshold factors, which become irrelevant for $Q^2 \gg 4M_i^2$, and illustrate our method using two quark families, u, d, s, and c. Then

$$N_f = \sum e_i^2 = \frac{10}{9}.$$

The P_{ij} are the NLO splitting functions for quarks and gluons. The formal expressions for these functions are fully known in the NLO [20].

We first insert the hard Pomeron behavior of the parton distribution functions (PDFs) in the DGLAP evolution equations. After integrating we find a set of coupled formulas to extract the gluon distribution and the singlet structure function

$$\begin{aligned}
\frac{dG}{dt} &= \frac{\alpha_s}{2\pi}\left[G(x,t)\eta_1+\Sigma(x,t)\beta_1\right],\\
\frac{d\Sigma}{dt} &= \frac{\alpha_s}{2\pi}\left[G(x,t)\eta_2+\Sigma(x,t)\beta_2\right],
\end{aligned} \tag{2}$$

where

$$\begin{aligned}
\eta_1 &= \frac{2C_A(1-x^{\lambda_g})+\dfrac{\alpha_s}{2\pi}(12C_FN_fT_R-46C_AN_fT_R)(1-x^{\lambda_g})}{\lambda_g},\\
\beta_1 &= \frac{2C_F(1-x^{\lambda_s})+\dfrac{\alpha_s}{2\pi}(9C_FC_A-40C_FN_fT_R)(1-x^{\lambda_s})}{\lambda_s},\\
\eta_2 &= \frac{\dfrac{\alpha_s}{2\pi}40C_AN_fT_R(1-x^{\lambda_g})}{\lambda_g}, \quad \beta_2 = \frac{\dfrac{\alpha_s}{2\pi}40C_FN_fT_R(1-x^{\lambda_s})}{\lambda_s}.
\end{aligned} \tag{3}$$

For the $SU(N)$ gauge group, we have

$$C_A = N, \quad C_F = \frac{N^2-1}{2N}, \quad T_F = N_f T_R, \quad T_R = \frac{1}{2},$$

where C_F and C_A are the color Casimir operators. In the NLO, the running coupling constant $\alpha_s/2\pi$ has the form

$$\frac{\alpha_s}{2\pi} = \frac{2}{\beta_0 t}\left[1 - \frac{\beta_1 \ln t}{\beta_0^2 t}\right] \tag{4}$$

with

$$\beta_0 = \frac{1}{3}(33 - 2N_f), \quad \beta_1 = 102 - \frac{38}{3}N_f,$$

and the variable t is defined by

$$t = \ln\left(\frac{Q^2}{\Lambda^2}\right)$$

and Λ is the QCD cut-off parameter.

We now combine terms and define a relation between exponents of the gluon and singlet distributions. According to the Regge theory, the high-energy (low-x) behavior of both gluons and sea quarks is controlled by the same singularity factor in the complex angular momentum plane [6], and we therefore expect

$$\lambda_s = \lambda_g = \lambda.$$

We have fitted exponents to a power law in the low-x limit that we took for the PDFs. In the Regge theory, the high-energy behavior of hadron–hadron and photon–hadron total cross sections is determined by the pomeron intercept

$$\alpha_P = 1 + \lambda,$$

and is given by

$$\sigma^{tot}_{\gamma(h)p}(\nu) \propto \nu^{\lambda}.$$

This behavior is also valid for a virtual photon for $x \ll 1$, leading to the well-known behavior

$$F_2 \propto x^{-\lambda}$$

of the structure functions at fixed Q^2 as $x \to 0$ [21–23]. The power of λ is found to be either $\lambda = 0$ or $\lambda = 0.5$. The first value corresponds to the soft Pomeron and the second value to the hard (Lipatov) Pomeron intercept. The form $x^{-\lambda_g}$ of the gluon parameterization at small x is suggested by Regge behavior, but because the conventional Regge exchange is that of a soft Pomeron, with $\lambda_g \sim 0$, we may also allow a hard Pomeron with $\lambda_g \sim 0.5$.

The form $x^{-\lambda_s}$ in the sea-quark parameterization comes from similar considerations because the process $g \to q\overline{q}$ dominates the evolution of the sea quarks at small x. Hence the fits to early HERA data have as the constraint $\lambda_s = \lambda_g = \lambda$, because the value of λ should be close to 0.5 in quite a broad range of low x [4, 7–9, 24].

After successive differentiations of both sides of Eqs. (2), multiplication by $G^{-1}(x,t)$, and some rearrangments, we find independent inhomogeneous second-order differential equations for λ_g and λ_s as functions of t:

$$\frac{2\pi}{\beta_1\alpha_s}\ln x\frac{d^2\lambda_g}{dt^2} - \left[\frac{\eta_1+\beta_2}{\beta_1} - 2\pi\frac{d(\beta_1\alpha_s)^{-1}}{dt} + \right.$$
$$+ \frac{2\pi}{\beta_1\alpha_s}\ln x\frac{d\lambda_g}{dt}\left]\left[\ln x\frac{d\lambda_g}{dt} + \right.\right.$$
$$\left.\left. + \frac{d(\eta_1\beta_1^{-1})}{dt} - \frac{\alpha_s}{2\pi}\left(\frac{\eta_1\beta_2}{\beta_1} - \eta_2\right)\right] = 0 \tag{5}$$

and

$$\frac{2\pi}{\eta_2\alpha_s}\ln x\frac{d^2\lambda_s}{dt^2} - \left[\frac{\eta_1+\beta_2}{\eta_2} - 2\pi\frac{d(\eta_2\alpha_s)^{-1}}{dt} + \right.$$
$$+ \frac{2\pi}{\eta_2\alpha_s}\ln x\frac{d\lambda_s}{dt}\left]\left[\ln x\frac{d\lambda_s}{dt} + \frac{d(\beta_2\eta_2^{-1})}{dt} - \right.\right.$$
$$\left.\left. - \frac{\alpha_s}{2\pi}\left(\frac{\eta_1\beta_2}{\eta_2} - \beta_1\right)\right] = 0. \tag{6}$$

The presented results give independent evolution equations for the gluon and also the singlet structure function exponents at small x. These equations show that the exponents are functions of Q^2. The $\ln Q^2$ dependence of the exponents has a second-degree polynomial behavior. By solving these evolution equations, we can determine exponents with the starting parameterizations of exponents

$$\lambda_i(t_0) = \frac{d\ln f_i(x,t_0)}{d\ln(1/x)}$$

respectively given by the input distribution of the partons and its derivatives [25–28]. Therefore, the effective power-law behavior of the gluon distribution and the singlet structure function corresponds to

$$f_i(x,t) = f_i(x,t_0)x^{-(\lambda_i(t)-\lambda_i(t_0))}, \quad i = \Sigma, g. \tag{7}$$

If we want to perform parton distribution functions, we need to fix these at the initial scale

$$t_0 = \ln\frac{Q_0^2}{\Lambda^2}.$$

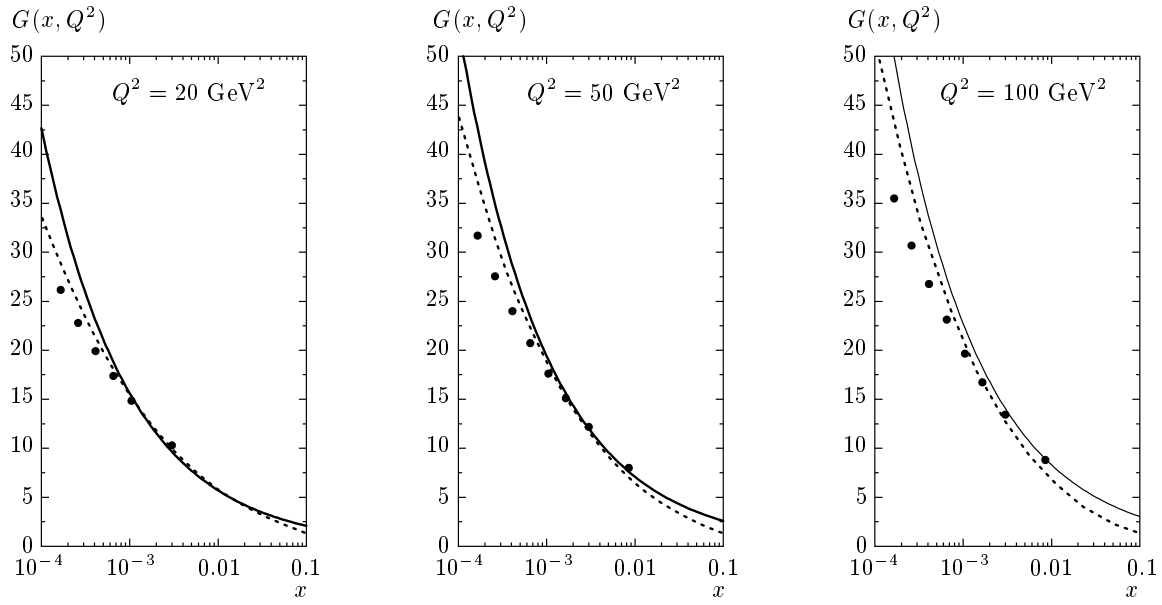

Fig. 1. The gluon distribution vs. x at fixed Q^2 values (circles) compared with the DL fit [7, 28] (solid lines) and the GRV parameterization [27] (dashed lines)

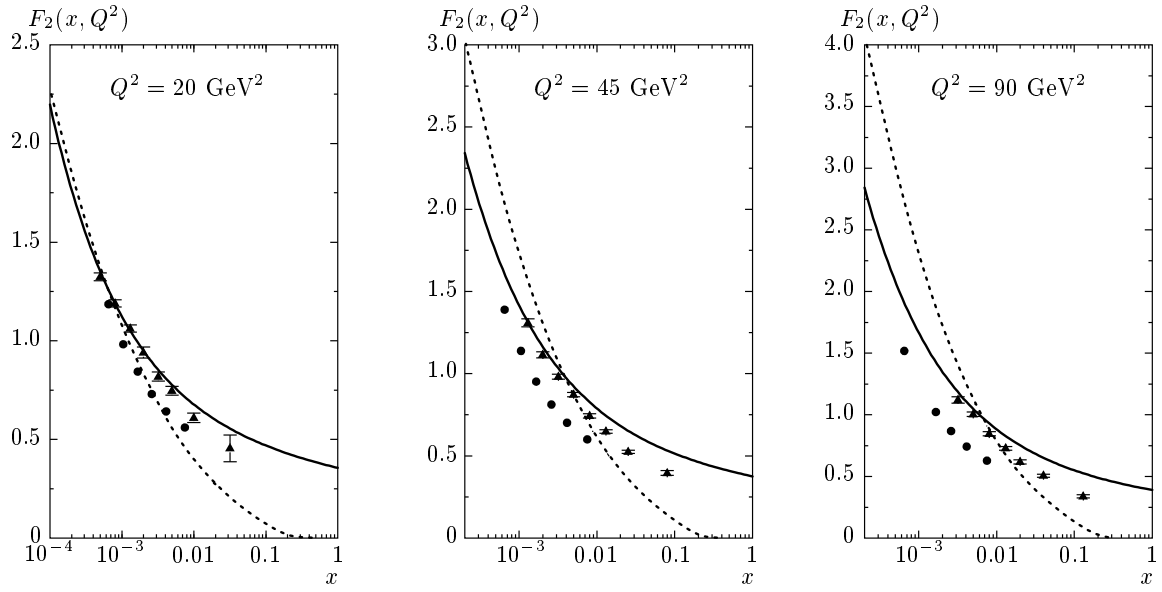

Fig. 2. The calculated values of the structure function F_2 for several values of Q^2 plotted as a function of x with the starting parameterization of the structure function at $Q_0^2 = 5$ GeV^2 (circles), compared with the next-to-leading-order QCD fit to the H1 data with total errors (triangles), and also with the DL fit [7, 28] (solid lines). The dashed lines represent the results in [23] for the GRV parameterization of the gluon distribution function and the parton structure function

Here, we used the QCD cut-off parameter $\Lambda^4_{\overline{MS}} = 0.323$ GeV [11] for $\alpha_s(M_{z^2}) = 0.119$. In our calculations, we also need the initial conditions $f_i(x,t_0)$ and $\lambda_i(t_0)$ that correspond to the input parameterization. To test the validity of our gluon distribution, we calculate the gluon (or singlet) distribution functions and exponent of the gluon (or singlet) distribution using Eq. (7) and compare them with the theoretical predictions starting with the evolution at $Q_0^2 = 5$ GeV^2. The results of calculation are shown in Figs. 1 and 2 at se-

veral Q^2 values. As can be seen from these figures, the values of $f_i(x,Q^2)$ increase as x decreases. In these figures, we compare our results for the gluon distribution function and for the proton structure function with the Donnachie–Landshoff (DL) fit [7, 28] and H1 data [25] with the total errors at Q^2 values. Also, we compared our predictions for the proton structure function with Ref. [23]. The proton structure function corresponds to the gluon distribution function at $x_g \approx 2x$ upon integration of the DGLAP equation. In this integration, we used from the standard Gluk–Reya–Vogt (GRV) parameterizations. We have taken the DL parametric form for the starting distribution at $Q_0^2 = 5$ GeV^2 given by

$$xg(x,Q^2) = 0.95(Q^2)^{1+\epsilon_0}(1+Q^2/0.5)^{-1-\epsilon_0/2}x^{-\epsilon_0},$$

where $\epsilon_0 = 0.437$ according to a hard-Pomeron exchange. We can see that these distribution function values increase as x decreases, but with a somewhat smaller rate. This behavior is associated with the exchange of an object known as the hard Pomeron. Having concluded that the data for F_2 require a hard-pomeron component, it is necessary to test this with our results, as in Fig. 2.

To conclude, we have obtained independent solutions for the gluon and singlet exponents based on the DGLAP evolution equations with respect to the Regge behavior in the next-to-leading order at low x. Careful investigation of our results shows an agreement with the previously published parton distributions based on QCD. The gluon distribution and singlet structure functions increase as usual, as x decreases. The form of the obtained distribution functions for the gluon distribution and the singlet structure functions are similar to the one predicted from the parton parameterization. The formulas used to generate the parton distributions are in agreement with the increase observed in H1 experiments. These results also show that the exponents increase nonlinearly with respect to $\ln Q^2$ as x decreases. The behaviors of the distribution functions at low x are consistent with a power-law behavior. The obtained results give strong indications that the proposed formulas, being very simple, provide relatively accurate values for the gluon distribution and structure functions.

REFERENCES

1. Yu. L. Dokshitzer, Sov. Phys. JETP **46**, 641 (1977); G. Altarelli and G. Parisi, Nucl. Phys. B **126**, 298 (1997); V. N. Gribov and L. N. Lipatov, Sov. J. Nucl. Phys. **28**, 822 (1978).
2. L. F. Abbott, W. B. Atwood, and A. M. Barnett, Phys. Rev. D **22**, 582 (1980).
3. A. M. Cooper-Sarkar, R. C. E. Devenish, and A. De-Roeck, Int. J. Mod. Phys. A **13**, 3385 (1998).
4. A. K. Kotikov and G. Parente, Phys. Lett. B **379**, 195 (1996); J. Kwiecinski, arXiv:hep-ph/9607221.
5. R. D. Ball and S. Forte, Phys. Lett. B **335**, 77 (1994); Phys. Lett. B **336**, 77 (1994).
6. P. D. Collins, *An Introduction to Regge Theory and High-Energy Physics*, Cambridge University Press, Cambridge (1997).
7. A. Donnachie and P. V. Landshoff, Phys. Lett. B **296**, 257 (1992).
8. P. Desgrolard, M. Giffon, E. Martynov, and E. Predazzi, Eur. Phys. J. C **18**, 555 (2001).
9. P. Desgrolard, M. Giffon, and E. Martynov, Eur. Phys. J. C **7**, 655 (1999).
10. M. B. Gay Ducati and V. P. B. Goncalves, Phys. Lett. B **390**, 401 (1997).
11. K. Pretz, Phys. Lett. B **311**, 286 (1993); Phys. Lett. B **332**, 393 (1994).
12. A. V. Kotikov, arXiv:hep-ph/9507320.
13. C. Lopez and F. J. Yndurain, Nucl. Phys. B **171**, 231 (1980).
14. C. Lopez, F. Barreiro, and F. J. Yndurain, Z. Phys. C **72**, 561 (1996).
15. K. Adel, F. Barreiro, and F. J. Yndurain, Nucl. Phys. B **495**, 221 (1997).
16. G. Soyez, Phys. Rev. D **67**, 076001 (2003).
17. L. Csernai et al., Eur. Phys. J. C **24**, 205 (2002).
18. G. Soyez, Phys. Rev. D **71**, 076001 (2005).
19. G. R. Boroun and B. Rezaie, Phys. Atom. Nucl. **71**, 1076 (2008); G. R. Boroun, Zh. Exp. Teor. Fiz. **133**, 805 (2008).
20. R. K. Ellis, W. J. Stirling, and B. R. Webber, *QCD and Collider Physics*, Cambridge University Press, Cambridge (1996).
21. N. Nikolaev, J. Speth, and V. R. Zoller, Phys. Lett. B **473**, 157 (2000).
22. R. Fiore, N. Nikolaev, and V. R. Zoller, Pis'ma v Zh. Eksp. Teor. Fiz. **90**, 319 (2009).

23. I. P. Ivanov and N. Nikolaev, Phys. Rev. D **65**, 054004 (2002).

24. A. D. Martin, M. G. Ryskin, and G. Watt, arXiv:hep-ph/0406225.

25. C. Adloff et al., ($H1$ Collab.), Eur. Phys. J. C **21**, 33 (2001); Phys. Lett. B **520**, 183 (2001).

26. A. M. Cooper-Sarkar and R. C. E. D. Evenish, Acta. Phys. Polon. B **34**, 2911 (2003).

27. M. Gluk, E. Reya, and A. Vogt, Z. Phys. C **67**, 433 (1995); Eur. Phys. J. C **5**, 461 (1998).

28. P. V. Landshoff, arXiv:hep-ph/0203084.